PAPER • **OPEN ACCESS**

Natural Isotopic Activity Ratios as Evidence of Migration and Leaching of Uranium in Egyptian Granitic Rocks

Journal of Physics: Conference Series **2830** (2024) 012022 doi:10.1088/1742-6596/2830/1/012022

Natural Isotopic Activity Ratios as Evidence of Migration and Leaching of Uranium in Egyptian Granitic Rocks

Nahla A. Ismaiel[1], Eman Y. Frag[2], W. M. Seif[3], Hamed I. Mira[4], Ahmed M. Shabasy[5], Mahmoud R. Khattab[4*]

[1] Radiation Protection Department, Nuclear Power Plants Authority (NPPA), Cairo, Egypt
[2] Chemistry Department, Faculty of Science, Cairo University, Giza 12613, Egypt
[3] Physics Department, Faculty of Science, Cairo University, Giza 12613, Egypt
[4] Geochemical Exploration Department, Nuclear Materials Authority, Cairo, Egypt
[5] Nuclear and Radiological Safety Research Centre (NRSRC), Egyptian Atomic Energy Authority (EAEA), Nasr City, Cairo 11762, Egypt

mahmoudkhattabnma@yahoo.com

Abstract. Gamma-spectrometry was utilized to analyse radionuclides in granitic rocks from the El Eridiya area through radiometric measurements. The activity concentration of ^{238}U ranges from 3493±83 to 5209±104 Bq kg^{-1}, while for ^{234}U and its isotope (^{235}U), it varies from 957±32 to 1012±34 Bq kg^{-1} and 153.0±4.5 to 256.0±5.5 Bq kg^{-1}, respectively. However, for the isotopes ^{230}Th and ^{232}Th, the range is from 11217±254 to 16291±305 Bq kg^{-1} and 31.0±1.1 to 85.3±0.5 Bq kg^{-1}, respectively. The activity concentration of 40K ranged from 67.9±1.6 to 109.0±2.1 Bq kg^{-1}. The ratios of ^{234}U/^{238}U in the studied granitic rock samples vary from 0.21±0.01 to 0.54±0.03. Due to the current oxidising conditions, most of the rock samples show a higher presence of ^{234}U compared to ^{238}U, with ^{234}U/^{238}U activity ratios below one. Additionally, the activity ratios of ^{232}Th/^{238}U range from 0.006 to 0.019 in the granitic rock samples from the El Eridiya area. Figures 3 and 4 display uranium enrichment, with all samples showing ^{232}Th/^{238}U ratios below one for the earth's crust. Additionally, all samples showed ^{230}Th/^{238}U and ^{230}Th/^{234}U activity levels above one, suggesting preferential leaching of uranium in an oxygen-rich setting. Similarly, the ^{234}U/^{238}U and ^{230}Th/^{238}U activity ratios are below and above one, indicating U-leaching and U-accumulation, respectively. Figure 3 and 4 show uranium enrichment, with all samples having ^{232}Th/^{238}U activity ratios below one for the earth's crust. There were benefits to uranium leaching in an environment with oxidation in all samples, with ^{230}Th/^{238}U and ^{230}Th/^{234}U activity ratios exceeding one. If the ^{234}U/^{238}U activity ratio is lower than one but the ^{230}Th/^{238}U activity ratio is higher than 1, it suggests U-leaching; if the ^{234}U/^{238}U activity ratio is greater than one and the ^{230}Th/^{238}U activity ratio is less than 1, it suggests U-accumulation.

Keywords: Granites; Radioactivity; Radionuclides; Migration; Leaching; Isotopes.

1. Introduction

Granites, formed by molten magma deep underground, contain high levels of uranium and thorium, leading to increased radiation levels. These igneous rocks naturally have large amounts of uranium and thorium, contributing to their radiation levels [1, 2]. The terrestrial radioisotopes in granitic rocks, along with the resulting products, typically differ based on their origin. Granite, commonly used in housing and decoration, contains natural radionuclides like ^{40}K, ^{232}Th, ^{238}U, and ^{226}Ra. Assessing these levels is crucial in evaluating radiation risks to the public. Measurements of radioactive concentration dispersion will aid in establishing regulations for the management and use of these rocks [3]. It is common knowledge that uranium and thorium are valuable indicators for monitoring the movement of radionuclides in the uranium series and underground fluids in varied aquifer circumstances. Their presence has been widely applied in geological, marine, and environmental research. Two primary techniques for the enrichment of uranium and thorium are partial melting and fractional crystallization [4]. Between ^{217}U and ^{243}U, there are twenty-seven known uranium isotopes. ^{221}U has the shortest half-life at 700 nanoseconds. However, there are naturally occurring uranium radioisotopes with long half-lives, such as ^{238}U (99.27%; 4.47×10^{9} years), ^{235}U (0.72%; 7.04×10^{8} years), and ^{234}U (0.0057%; 2.45×10^{5} years). Uranium also has different isomers. The main decay mechanism of uranium isotopes, including beta decay, is influenced by atomic absorption, spontaneous fission, and electron capture [5]. Isotopes ^{234}U and ^{238}U are part of the radioactive decay chain of ^{238}U, with ^{238}U as the parent nuclide and belonging to the uranium-radium family. Four thorium isotopes found in nature are ^{228}Th, ^{230}Th, ^{232}Th, and ^{234}Th, making up 8×10^{-4} % of the earth's crust. ^{228}Th and ^{234}Th are produced from decays of ^{228}Ra and ^{238}U, respectively. ^{230}Th from ^{234}U can have an authigenic or terrigenous origin. ^{232}Th originates from detrital or weathered terrigenous minerals, with detrital Th potentially lingering in particulates while authigenic Th can be eliminated quickly by settling particles [6, 7].

The mineral and chemical composition, as well as redox potentials, are likely factors influencing the presence of uranium and thorium isotopes in rocks, with Hexavalent uranium being more readily dissolved [8]. Differences in the chemical and physical properties of various elements within the radioactive series may cause an imbalance, resulting in alterations in erosion and levels of radioactivity. Furthermore, the presence of both ^{222}Rn and ^{220}Rn in different samples, along with α- and β-decay in other nuclei, can disrupt the crystal structure. The ratio of radioactivity between ^{234}U and ^{230}Th nuclei remains constant, with activity ratios of ^{234}U/^{238}U, ^{230}Th/^{234}U, and ^{230}Th/^{238}U staying steady. Yet, changes in atmospheric and groundwater circulation can impact the system, leading to modifications in its physicochemical state, which may result in fragmentation and fluctuations in activity levels. This data can be used to evaluate options for underground pollutants or to rehabilitate environments affected by redox activities [9].

2. Materials and Method

2.1. Geological Setting

El Eridia area is primarily composed of Precambrian basement rocks, with Nubian sandstone covering the west (Figure 1). Ophiolite is the oldest rock, followed by metavolcanic, diorite, and granodiorite rocks. The area includes granite, felsite, jasper veins, and meta granites with mineral deposits. The El Eridia pluton covers about 70 km and is surrounded by altered rocks, faults, and fractures. Alteration features include silicification, kaolinization, sericitization, chloritization, and carbonatization. Uranium mineralization is linked to hydrothermal alteration in granite areas. Uranium mineralization occurs in cracked regions with jasperoid veins in the siliceous veins [4].

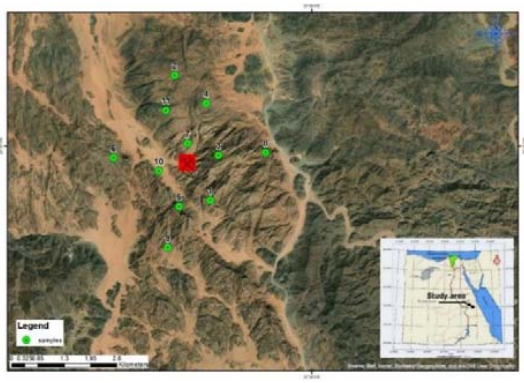

Figure 1. Geologic map of El Aradiya area and locations of collected samples.

The felsite veins only cut through the older granite, which can range in size from a few meters to more than 10 km long and up to 5 meters in width. This suggests that the dikes were created before the younger granites were laid down. Small to medium outcrops often display exfoliation and a gneissic texture, characteristic of the oldest granites. In the northern regions, certain rocks may exhibit black and white bands, resembling migmatite. The most ancient granites are categorized according to their mineral composition, including quartz diorite, tonalite, and granodiorite. Quartz diorite contains less quartz and more plagioclase than tonalite and granodiorite. Tonalite and granodiorite contain moderate amounts of quartz and a variety of plagioclase and potassium feldspar. The amount of biotite is lower in tonalite and granodiorite when compared to quartz diorite. Hornblende is not abundant in any of the three categories [10]. The oval pluton's younger granites consist mostly of monzogranite and syenogranite, featuring a significant amount of quartz. They originated between 568 ± 17 Ma and 603-575 Ma in the aftermath of Eastern Desert's tectonic activities. Monzogranite, syenogranite, and modified granite have different mineral compositions, characterized by different proportions of quartz, plagioclase, and biotite. Muscovite is exclusively located in syenogranite and modified granite [11, 12].

2.2. Analytical method

2.2.1. Gamma Spectrometry. To keep a balance in radioactive decay sequences and avoid contamination from radionuclides ^{222}Rn and ^{220}Rn, sample containers were tightly sealed and kept for at least one month [4]. The specimens were analysed using a high-purity germanium (HPGe) gamma ray detector that has a relative efficiency of 60 %. Three standard and reference materials (RGU^{-1}, $RGTh^{-1}$, and RGK^{-1}) from the International Atomic Energy Agency (IAEA) were used to determine the measuring efficiency of ^{238}U, ^{232}Th, and ^{40}K activity. Taking into account the self-absorption effects of the gamma photon source and utilizing specific radionuclide techniques helped minimize the uncertainty in gamma ray intensities [13]. Using the γ-lines of its daughter isotopes ^{234}Th and ^{234}mPa, concentrations of ^{238}U were determined by utilizing the energy levels of 63.3 and 1001 KeV [14].

The analysis of 53.2 and 120.9 keV γ-lines was used to determine the activity concentration of ^{234}U. The activity concentration of ^{232}Th was determined by measuring the γ-rays emitted by ^{228}Ac at 338.4 keV and 911.2 keV, and by ^{208}Tl at 583 keV and 2614.4 keV. The concentration of ^{226}Ra's activity includes its daughter isotopes ^{220}Rn, ^{214}Pb, and ^{214}Bi. Measurement of ^{40}K activity concentration was done using its γ-line located at 1460.8 keV. Activity concentrations are typically calculated with an uncertainty of less than 10% on average. Gamma rays emitted by ^{214}Bi and ^{214}Pb may suggest the existence of ^{226}Ra indirectly. The activity concentration of ^{214}Pb was measured by detecting γ-rays at 241.9, 295.2, and 351.9 keV, while the activity concentrations of ^{214}Bi and ^{210}Pb were determined using γ-rays at 609.3 and 46.5 keV [15]. The levels of ^{235}U were measured with γ-rays at different energies: 143.8 keV (with 10.5 % intensity), 163.4 keV (4.8 % intensity), and 205.3 keV. The activity concentration of ^{235}U (10.96 %) was determined using the peak area at 143.76 keV. The peak at 185.72 keV accounted for 57.2 % of the total area attributed to ^{235}U. The ^{226}Ra area was determined by subtracting the area of the peak at 186 keV from the area of the ^{235}U peak. These calculations took into account proportion, productivity, and gamma radiation levels.

2.3. Environmental Hazard Impacts Calculations

2.3.1. Absorbed Dose Rate in Air (D). The formula was used to calculate the gamma dose rates measured in the air at a distance of 1 meter from the ground. This method took into account an even spread of the radionuclides ^{226}Ra, ^{232}Th, and ^{40}K.

$$\mathbf{D\ (nGy.h^{-1}) = 0.462A_{Ra} + 0.604A_{Th} + 0.0417A_K} \quad \textbf{(1)}$$

which provided by UNSCEAR, 2000 [17] and Khandaker et al., 2019 [18]. Here, A_{Ra}, A_{Th} and A^K represent the average specific activities of ^{226}Ra, ^{232}Th and ^{40}K in Bq kg^{-1}, respectively.

2.3.2. Annual Effective Dose Equivalent (AEDE). Workers, visitors, and residents in the vicinity were assessed for their exposure to radiation by determining the average absorbed dose rates (ADR). These rates were then utilized to compute the annual effective dose equivalent (AEDE) in μSv.yr^{-1}. The AEDE was derived from the absorbed dose using equation 2 [19].

$$\mathbf{AEDE\ (\mu Sv.yr^{-1}) = D\ x\ T\ x\ OF\ x\ 10^{-3}} \quad \textbf{(2)}$$

where T is total time in hours per year; 8760 and OF is the occupancy factor. For this work, an outdoor occupancy factor of 0.2 was used [20].

2.3.3. Radium Equivalent Activity (Ra_{eq}). The exposure to radiation can be defined in terms of the radium equivalent activity (Raeq), which can be expressed by the following equation 3;

$$\mathbf{Ra_{eq} = A_{Ra} + 10/7A_{Th}+10/130A_K} \quad \textbf{(3)}$$

where A^{Ra}, A^{Th} and A^K are the specific activities of Ra, Th and K, respectively, in Bq.kg^{-1}.

2.3.4. External and Internal Hazard Index (H_{ex} and H_{in}). To limit the annual external gamma-ray dose to 1.5 Gy for the samples under investigation equation [22], the external hazard index (H_{ex}) is given by,

$$\mathbf{H_{ex} = A_{Ra}/370 + A_{Th}/259 + A_K/4810} \quad \textbf{. (4)}$$

The internal exposure to ^{222}Rn and its radioactive progeny is controlled by the internal hazard index (H_{in}) and calculated from equation 5 as,

$$\mathbf{H_{in} = A_{Ra}/185 + A_{Th}/259 + A_K/4810} \quad \textbf{.(5)}$$

These indices must be lower than unity in order to keep the radiation hazard insignificant [18].

2.3.5 Gamma Index (I_γ). Another radiation hazard index called the representative level index, Iγ, is calculated from equation 6 as follows;

$$\mathbf{I_\gamma = A_{Ra}/150 + A_{Th}/100 + A_K/1500} \quad \textbf{(6)}$$

where A_{Ra}, A_{Th} and A_K are the activity concentrations of ^{226}Ra, ^{232}Th and ^{40}K, respectively in Bq.kg^{-1}. The safety value for this index is ≤ 1.

3. Results and Discussions

3.1. Radionuclides Distributions

Table 1 shows ^{238}U activity concentrations ranging from 3493±83 to 5209±104 Bq kg^{-1} and ^{234}U activity concentrations ranging from 957±32 to 1012±34 Bq kg^{-1}. Different thorium isotopes showed varying activity concentrations of ^{230}Th ranging from 11217±254 to 16291±305 Bq kg^{-1}, and for ^{232}Th concentrations varied from 31±1.1 to 85.3±0.5 Bq kg^{-1} (Table 1). Activity concentrations of ^{235}U in granite rock samples varied between 153±4.5 and 256±5.5 Bq kg^{-1}, with ^{40}K activity concentrations ranging from 67.9±1.6 to 109±2.1 Bq kg^{-1} (Table 1). The findings indicate that the radionuclide levels in the gathered samples exceed the worldwide average levels of 33, 45, and 412 Bq kg^{-1} for ^{238}U, ^{232}Th, and ^{40}K, respectively (Figure 2).

The samples analysed contain shear zone dikes with silica, microgranite, and uranium. This composition is linked to the high ^{238}U concentration. The samples are from uranium-rich granite. Radioactivity levels can increase when uranium and thorium are in heavy minerals like zircon, fluorite, and apatite, as well as in minerals like uraninite, thorianite, and monazite, commonly found in granite and basalt rocks.

3.2. Isotopic activity concentrations

^{234}U is generally in balance with ^{238}U, although discrepancies may arise due to selective leaching in groundwater, oceans, lakes, rivers, and soils. In the natural environment, uranium is present in two oxidation states: U(IV) and U(VI). Under marine conditions that promote oxidation, U(VI) becomes mobile and forms soluble complexes by combining with carbonate and phosphate. In reducing conditions, uranium exists as U(IV) and forms less soluble compounds with hydroxides, hydrated fluorides, and phosphates. The gathered granite rock samples showed $^{234}U/^{238}U$ activity ratios that varied between 0.21±0.01 and 0.54±0.03 (Table 1). All rock samples had $^{234}U/^{238}U$ activity ratios below one (Figure 3), showing ^{234}U is more easily mobilized than ^{238}U from the rock under oxidation conditions. The $^{232}Th/^{238}U$ activity indices for granite rocks in the El Eridiya area varied between 0 and 0.006±0.0, and 0.019±0.0 (Table 1). It is interesting to note that all samples exhibited values below one for the $^{232}Th/^{238}U$ ratio within the earth's crust, suggesting a higher concentration of uranium. Moreover, a $^{230}Th/^{238}U$ activity ratio of 300,000 was calculated, showing the time required for ^{230}Th to reach its equilibrium activity when the $^{234}U/^{238}U$ activity ratio is one. It is important to note that all samples showed $^{230}Th/^{238}U$ and $^{230}Th/^{234}U$ activity ratios higher than one, indicating a preference for uranium leaching in an oxidized environment. (Figure 3) depicted in the image. The presence of more ^{230}Th than ^{238}U in the suspended sediments of indicates that uranium is more likely to move faster than thorium during erosion. Studies on selective mining have also indicated that secondary iron ores hinder the migration of uranium and thorium isotopes.

Table 1. The activity concentrations of different radionuclides and isotopic activities ratios

Nuclides / Samples	1	2	3	4	5	6	7	8
^{238}U Series								
^{234m}Pa	4817±101	4458±96	5252±105	4114±91	5198±104	3866±87	4458±94	5209±104
^{234}U	2159±50	1771±45	1474±41	1452±22	1232±18	1334±38	957±32	1345±39
^{230Th}	14604±291	14354±268	16291±305	14281±282	16121±301	13953±274	14550±281	11217±254
^{226}Ra	10105±385	10223±388	9778±120	10111±377	10017±294	10416±377	10186±195	10415±384
^{214}Pb	4140±10	6225±12	4863±11	5063±12	4241±5	5410±12	4153±10	4618±11
^{214}Bi	5001±55	4880±25	4331±24	4687±25	4574±13	5009±25	4784±24	4847±25
^{232}Th Series								
^{228}Ac	47.8±1.5	136.4±2.6	53±1.6	24.8±1.2	34.9±2.2	67±1.7	84.8±1.7	35.4±1.3
^{208}Tl	28.6±0.8	34.2±0.9	29.8±0.9	27.5±0.8	33.6±0.8	21.9±0.7	28.5±0.8	26.3±0.8
Average	38.2±1.2	85.3±0.5	41.4±1.3	26.2±1	34.3±1.5	44.5±1.2	57±1.3	31±1.1
^{235}U	213.5±3.2	222.7±5.8	256±5.5	208±4.8	238±5.4	178±6.3	208±5.4	235±6.3
^{40}K	104±2.1	111.8±2.17	103±2.1	93.1±1.9	82.7±1.7	99.8±1.9	109±2.1	107±2.1
$^{238}U/^{235}U$	22.5±0.7	2۰.8±0.6	20.5±0.9	19.7±0.6	21.8±0.7	21.7±0.7	21.4±1.8	22.2±1.6
$^{234}U/^{235}U$	10.1±0.8	7.9±0.3	14.3±0.9	7±0.2	5.18±0.4	7.6±0.6	4.6±0.3	5.7±0.5
$^{234}U/^{238}U$	0.45±0.01	0.39±0.01	0.28±0.02	0.35±0.01	0.24±0.03	0.35±0.02	0.21±0.01	0.26±0.02
$^{238}U/^{234}U$	2.23±0.01	2.52±0.02	3.56±0.02	2.83±0.04	4.22±0.07	2.89±0.06	4.7±0.08	3.87±0.07
$^{226}Ra/^{238}U$	2.1±0.05	2.30±0.04	1.86±0.05	2.45±0.06	1.93±0.05	2.96±0.08	2.28±0.08	1.99±0.07
$^{230}Th/^{238}U$	3.03±0.08	3.22±0.09	3.1±0.05	3.47±0.07	3.1±0.07	3.6±0.08	3.26±0.09	2.15±0.07
$^{226}Ra/^{230Th}$	0.69±0.01	0.71±0.01	0.6±0.03	0.71±0.02	0.62±0.03	0.75±0.04	0.7±0.04	0.93±0.05
$^{230}Th/^{234}U$	6.76±0.9	8.1±0.7	11.1±0.9	9.83±0.8	13.1±1.1	10.45±1.4	15.2±2.1	8.34±1.9
$^{232}Th/^{238}U$	0.008±0.0	0.019±0.0	0.008±0.0	0.006±0.0	0.007±0.0	0.012±0.0	0.013±0.0	0.006±0.0
U (ppm)	388.5	359.5	423	332	419	312	360	420
Th (ppm)	9.4	21	10.2	6.45	8.4	10.9	14.03	7.6
Th/U	0.02	0.06	0.02	0.02	0.02	0.03	0.38	0.02
U/Th	41.3	17.1	41.5	51.4	49.8	28.6	25.6	55.3

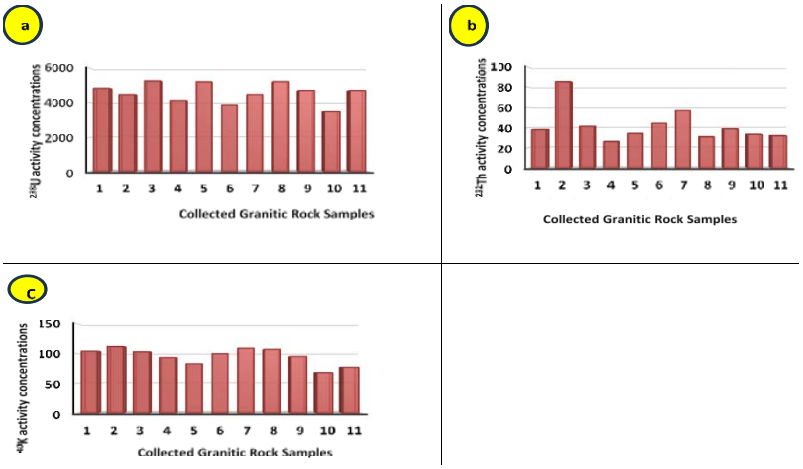

Figure 2. Distributions of ^{238}U, ^{232}Th and ^{40}K activity concentrations

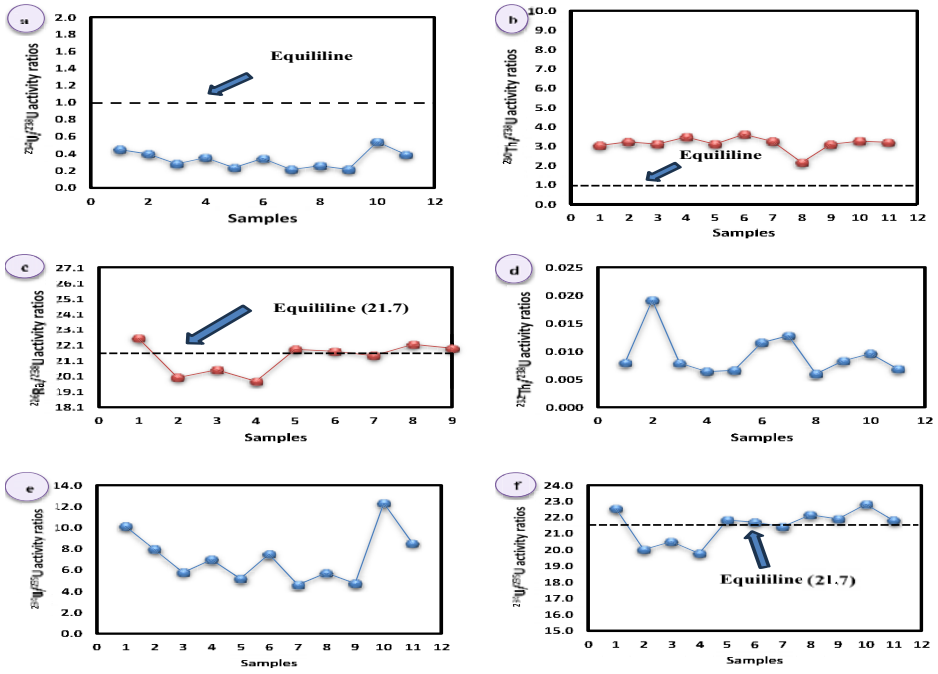

Figure 3. Variation of $^{234}U/^{238}U$, $^{230}Th/^{238}U$, $^{232}Th/^{238}U$, $^{234}U/^{235}U$ and $^{226}Ra/^{238}U$ activity ratios

The high level of ^{230}Th in a sample may result from either U loss or ^{230}Th gain through recoil implantation from decaying ^{234}U atoms in a solution. The reason some solids have higher $^{234}U/^{238}U$ and $^{230}Th/^{238}U$ activity ratios than one may be due to the immobility of Th in geochemistry. This occurrence is identified as $^{234}U+^{230}Th$ recoil. The primary reason for the radioactive imbalance between ^{230}Th and ^{234}U is the enhanced dissolution, resorption, and reprecipitation of ^{234}U resulting from α-decay. Colloids are closely linked to thorium isotopes. Table 1 and Figure 3 display the isotope activity rates of the

granite rock samples that were collected. These findings suggest that the separation of uranium isotopes was significantly influenced by redox processes. According to theory, U isotopes tended to be preserved in oxidized states like dissolved U^{6+}, while ^{238}U was more likely to be found in reduced forms like uraninite. The difference in ^{226}Ra and ^{238}U levels is due to the contrasting geochemical characteristics of these isotopes. Uranium can move around in oxidizing conditions as U(VI), but stays in place in reducing conditions like U(IV). On the other hand, the movement and restriction of the radius are affected by conflicting circumstances. Radium, found only in the +2-oxidation state, is trapped through coprecipitation and creation of solid solutions with divalent metal sulfate and carbonate minerals, as well as through adsorption onto other minerals. Radium is less likely to move around in oxidizing conditions compared to uranium because it binds strongly to clay and iron minerals typically found in those conditions after the host rock weathers. The $^{226}Ra/^{238}U$ activity ratio in groundwater was predicted to be lower in the oxidizing weathering zone compared to the reducing no climatic zone. The decrease in proportions may be due to the focus on U. The existence of imbalance caused by the migration of ^{226}Ra implies that the system remained open for 8,000 years. Except for sample 1, most samples had $^{230}Th/^{238}U$ activity ratios below one, showing that uranium was selectively leached or that ^{230}Th was leached by acidified water in rocks with high sulfur content. The rise in ^{230}Th levels in sample 1 may be attributed to the adsorption of ^{230}Th by clay minerals or iron oxides [17]. The Thiel diagram indicated that the activity ratios of the sandstone samples studied did not align with secular equilibrium, shown by the distortion of the $^{234}U/^{238}U$ and $^{230}Th/^{238}U$ ratios (Figure 4). Solid phase equilibrium was identified through two methods: U accumulation leading to a decrease in the $^{230}Th/^{238}U$ ratio, and uranium leaching leading to an increase in the $^{230}Th/^{238}U$ ratio. The diagram's forbidden zone indicated unstable situations or reversible processes like accumulation and leaching [17]. Uranium leaching had a $^{234}U/^{238}U$ ratio < 1 and a $^{230}Th/^{238}U$ ratio > 1, whereas U enrichment had a $^{234}U/^{238}U$ ratio > 1 and a $^{230}Th/^{238}U$ ratio < 1. All samples of granite analyzed in this study were found to be located in the uranium leaching zone (Figure 4).

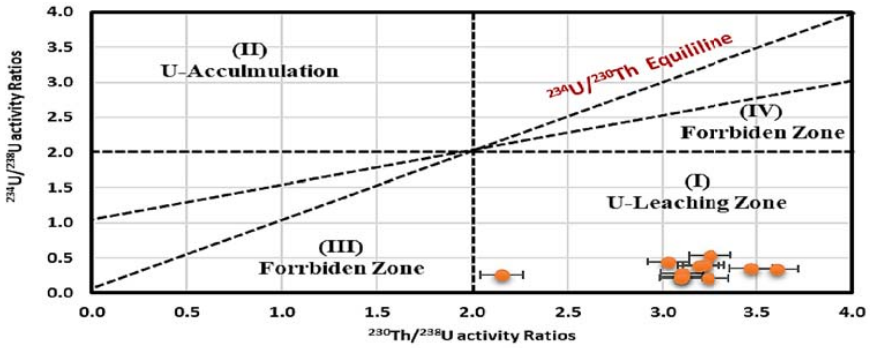

Figure 4. $^{234}U/^{238}U$ vs $^{230}Th/^{238}U$ activity ratio diagram the subsector marked as (I) and (III) forbidden zone, (II) leaching zone and (IV) accumulation zone.

3.3. Environmental Risk Assessments

The effects of the environmental risk on the outcomes of the examined region have been recorded in table 2. The mean absorbed dosage of ^{238}U in the gathered samples is 57 $nGyh^{-1}$, while the mean absorbed dosage in the collected samples is 4674.54 $nGyh^{-1}$, surpassing the global average value.

Table 2. Environmental hazard impacts of the studied granitic rock samples

Sample No.	Abs. Dose ^{238}U (nGy.h^{-1})	Eff. Dose (mSv.y^{-1})	Ra_{eq}	H_{ex}	H_{in}	I_γ
1	4725.26	5.80	10166.52	27.48	54.79	67.82
2	4812.23	5.90	10351.95	27.98	55.61	69.08
3	4576.09	5.62	9844.00	26.61	53.04	65.67
4	4716.04	5.79	10154.72	27.45	54.77	67.73
5	4673.44	5.73	10071.50	27.22	54.30	67.18
6	4870.82	5.98	10486.18	28.34	56.50	69.95
7	4776.38	5.86	10274.57	27.77	55.30	68.55
8	4864.93	5.97	10466.51	28.29	56.44	69.81
9	4782.82	5.87	10298.89	27.84	55.51	68.70
10	3736.00	4.58	8050.18	21.76	43.38	53.70
11	4885.88	6	10536.97	28.48	56.82	70.28
Min	3736.00	4.58	8050.18	21.76	43.38	53.70
Max	4885.88	6	10536.97	28.48	56.82	70.28
Average	4674.54	5.74	10063.82	27.20	54.22	67.13

Samples showed an annual effective dose of 4.58 to 6 mSvy^{-1}, with an average of 5.74 mSvy^{-1}, exceeding the global average of 0.48 mSvy^{-1} according to UNSCEAR, 2000 **[17]**. The activity radius equivalent ranged from 8050.18 to 10536.97 Bq kg^{-1}, with an average of 10063.82 Bq kg^{-1}, surpassing the allowable limit of 370 Bq kg^{-1}. The values of H_{ex} and H_{in} fluctuated between 21.76 and 28.48, with an average of 27.20, suggesting that they are not suitable for construction. The gamma activity index (Iγ) varied between 53.70 mSvy^{-1} and 70.28, averaging at 67.13 mSvy^{-1}, exceeding safety standards and concentration index. The connection between environmental dangers and levels of ^{238}U, ^{232}Th, ^{226}Ra, and ^{40}K in the area indicates their notable impact on health hazards. Group II displays higher activity levels of ^{238}U and ^{226}Ra, whereas group III specifically has elevated concentrations of ^{232}Th, highlighting their significance for the region's natural radioactivity.

4. Conclusion

Granite rocks and the products made from them frequently have different levels of terrestrial radioisotopes, which vary based on where they come from. Granite is frequently utilized in the construction and embellishment of residences. The levels of uranium and thorium isotopes are greatly affected by the rocks' mineralogy, as well as their chemical composition and redox potential. The proportions of $^{230}Th/^{234}U$ and $^{230}Th/^{238}U$ levels in suspended load and granitic samples need to exceed one, since thorium is very poorly soluble in oxidized environments, whereas hexavalent uranium is quite soluble. After a period of 1.7 million years, the nuclides ^{238}U, ^{234}U, and ^{230}Th will achieve radioactive equilibrium in enclosed geological systems, with the activity ratios of $^{234}U/^{238}U$, $^{230}Th/^{234}U$, and $^{230}Th/^{238}U$ all being equal to one. Nevertheless, the process of weathering and the movement of groundwater can result in fractionation, which can alter the activity ratios away from unity. The levels of ^{238}U activity varied from 3493±83 to 5209±104 Bq kg^{-1}, whereas the levels of ^{234}U activity varied from 957±32 to 1012±34 Bq kg^{-1}. Regarding the isotopes ^{230}Th and ^{232}Th, the activity concentrations ranged from 11217±254 to 16291±305 Bq kg^{-1} for ^{230}Th, and from 31±1.1 to 85.3±0.5 Bq kg^{-1} for ^{232}Th. The levels of ^{235}U activity varied between 153±4.5 and 256±5.5 Bq kg^{-1}. Between 67.9±1.6 and 109±2.1 Bq kg^{-1}, the activity concentrations fluctuated in the ^{40}K sample. The results show that the levels of radioactive elements in the granite samples are above the global averages of 33, 45, and 412 for ^{238}U, ^{232}Th, and ^{40}K.

References

[1] Tzortzis M and Tsertos H 2004 J. Environ. Radioact. 77, 325-338.
[2] Fallatah O and Khattab M R 2023 Minerals 13, 165.
[3] Xinwei L, Lingqing W, Xiaodan J, Leipeng Y and Gelian D 2005 Radiat. Prot. Dosim. 118, 352-359.
[4] Khattab M R 2022 Physics and Chemistry of The Earth, Parts A/B/C. 128, 103204.
[5] Kondev F G, Wang M, Huang W J, Naimi S and Audi G 2021 Chinese Physics C, 45, 3, 030001.
[6] Ault T, Gosen BV, Krahn S and Croff A 2016 Nucl. Technol. 194, 136-151
[7] Khattab M R, Tuovinen H, Lehto J, El Assay I E, El Feky M G and Abd El-Rahman M A 2017 Instrum Sci Technol 45, 338-348.
[8] Condomines M, Loubeau O and Patrier P 2007 Chem Geol 244, 304-315.
[9] Pan Z, Roebbert Y, Beck A, Bartova B, Vitova T, Weyer S and Bernier-Latmani R 2022. Environ Sci Technol 56, 1753-1762.
[10] Abu Dief A and El-Tahir M 2008 J. King Abdilaziz Univ. Earth Sci. Sec. Jeddah KSA 19, 85-97.
[11] Fullagar P D 1980 In: M J Salem and M T Busrewil (ed). The geology of Libya Acad Press Ill, 1051-1053.
[12] Greenberg J K 1981 Geological Society of America Bulletin, Part I, 92, 224-256.
[13] Stoulos S, Manolopoulou M and Papastefanou C 2003 Journal of Environmental Radioactivity 69, 225-240.
[14] Madkour H A, El-Taher A, Ahmed A N, Mohamed AW and El-Erian TM 2012 J Environ Sci Tech 5, 210-221.
[15] Abdel Halim MAK and El-Taher A 2014 J Radioanal Nucl Chem 299, 1949-1953.
[16] Al-Full Z Z and Khattab M R 2022 J. Environ Sci and Health Part A, 57, 376-385.
[17] UNSCEAR. 2000 United Nations: New York, NY, USA, 2000; Volume 1.
[18] Khandaker U M, Asaduzzaman K, Bin Sulaiman A F, Bradley D A and Isinkaya M O 2018 Mar. Pollut Bull 127, 654-663.